Proceedings 10th NUMGE 2023
10th European Conference on Numerical Methods in Geotechnical Engineering
Zdravkovic L, Kontoe S, Taborda DMG, Tsiampousi A (eds)

https://doi.org/10.53243/NUMGE2023-78

A three-dimensional numerical modelling of an underground gallery excavation considering the influence of sedimentary rock cross-anisotropy

P. Rapanakis[1] , B. Pardoen[1] , D. Branque[1] , J.S. Cornet[2] , G. Armand[2]

[1]*LTDS - UMR5513, ENTPE, Université de Lyon, Vaulx-en-Velin, France*
[2]*Meuse/Haute-Marne Underground Research Laboratory, R&D Division, Andra, Bure, France*

ABSTRACT: Clayey geomaterials are favourable underground media for radioactive waste disposal. In sedimentary geomaterials, an anisotropic behaviour depending on the loading direction is frequently observed. This paper investigates the effect of the inherent structural anisotropy of the Callovo-Oxfordian (COx) claystone on the construction of a single circular gallery at great depth. The rock matrix behaviour is assumed to follow a classical Drucker-Prager elastoplastic constitutive law with shear strength hardening in which anisotropy is implemented using the fabric tensor approach. The study focuses on a three-dimensional mechanical modelling of the short-term response of the clay rock, the shape and extent of the excavation damaged zone (EDZ) around the gallery using a plastic indicator and the convergence of the gallery walls. The model implementation is realised with the finite element analysis solver Code Aster. Simulations are performed for different in-situ stress states and comparisons are made based on the field observations. The results highlight the influence of anisotropy in the short-term extension of the plastic zone and trigger future prospects for complex numerical models.

Keywords: 3D numerical modelling; Structural anisotropy; Fabric tensor; Excavation damaged zone

1 INTRODUCTION

In the context of deep geological repository for the long-term management of radioactive waste, certain geological formations such as clay rocks are considered as suitable host media. In France, the Callovo-Oxfordian (COx) claystone whose properties are thoroughly studied by the French National Radioactive Waste Management Agency (ANDRA), serves as the ideal host formation.

In 2000, the Underground Research Laboratory (URL) located in the Meuse/ Haute-Marne (MHM) (Figure 1) is constructed to investigate the suitability of a deep geological disposal facility operating in the aforementioned claystone. The MHM URL is located in the Paris basin and its main level at -490 m lying between -420 m and -550 m. The rock is between carbonate formations of poor permeability. The research program's initial goal was to characterize the clay's confining properties and promote the suitability of the COx claystone not only for hosting the operation of a geological disposal but also for preventing a possible radionuclide migration (Delay et al., 2007).

Similar to other clays, the COx exhibits substantially favourable conditions for the long-term confinement of the nuclear wastes. It is a fined-grained sedimentary rock characterized by low permeability (between $5x10^{-20}$ to $5x10^{-21}$ m^2) and an anisotropic structure with quasi horizontal bedding planes. Its average porosity is approximately 18% ± 1% at the main level of the URL. At the clay rich unit of the COx formation, the mineralogical study showed a mixture of tectosilicates (20%), carbonates (20%–25%) and clay minerals (50%–55%) together with subordinate pyrite and iron oxides (3%). The clay minerals composition is relatively constant at 55% I/S (illite–smectite interstratified minerals), 30% illite and 15% kaolinite and chlorite (Armand et al., 2013).

It is well known that the excavation of underground tunnels has a major effect on the vicinity of openings and the rock's response can be quite complex. The effect usually relies on a plethora of factors such as the in-situ stress field, the material properties, the excavation method, the pore pressure and the long-term behaviour. In the case of COx, it is observed that unloading causes the generation of joint and shear fractures (Armand et al., 2014) developing close to the gallery and result into a severe change in the hydromechanical properties of the rock. Due to the importance of a geological storage facility, the study of the Excavation Damaged Zone (EDZ) around the openings is important.

In the framework of radioactive geological disposal defining the EDZ is relative to the permeability for safety calculation defined by Tsang et al. (2005). Thus, the present purely mechanical study aims to provide an efficient three-dimensional macroscopic model able to

reproduce mainly the plastic zone extent around single galleries in different stress states. This will provide a approximation of the EDZ, although there is no direct relation between plasticity and permeability. Furthermore, its goal is to highlight the influence of the anisotropy of the clay rock on the plastic zone.

Different orientations of galleries are modelled and the obtained numerical results are compared to those observed experimentally.

2 ANISOTROPIC BEHAVIOUR OF ROCKS

Often, sedimentary rocks are formed by deposition and exhibit a layered structure. Consequently, they tend to behave differently based on the loading direction. This phenomenon is called inherent anisotropy and is strongly connected to the material microstructure; therefore, it introduces a directional dependence of the rock's behaviour and strength characteristics.

Experimentally, research has been carried out on different anisotropic geomaterials. Abelev & Lade (2004) and Lade (2007) performed tests on dense sands, stressing the importance of the loading direction to the obtained results. Furthermore, sedimentary rocks have also been thoroughly studied (Abdi et al., 2015; Duveau et al., 1998; Nasseri et al., 2003; Niandou et al., 1997). The majority of outcomes indicate a substantial change in the strength of the material depending on the angle between the loading direction and the rock's bedding plane. For the COx clay rock, the maximum values of strength are reached for a loading parallel or normal to the bedding plane, whereas the minimum value occurs for an angle close to 45° (Zhang et al., 2019).

At a larger scale, the material anisotropy can also affect the fractures around underground galleries (Armand et al., 2014). The fractured zone developing around the opening is influenced not only by the orientation of the galleries but also the anisotropy of the claystone. In particular, extensional and shear fractures are observed close to the galleries, but only the shear fractures are propagating deeper in the rock.

Numerical implementation of material anisotropy is presented in the literature, notably in the work of Pardoen et al. (2015), and Souley et al. (2022) for the case of the COx claystone. Additionally for similar rocks, numerical modelling is performed by Pietruszczak et al. (2002), Djouadi et al., (2020) for the Tournemire shale and by Nguyen & Le (2015), Parisio et al., (2015) for the Opalinus clay. To describe the influence of the anisotropic nature of the rocks on their shear strength behaviour, different criteria were used in each study. Predominantly, the main methods used in literature involve either the fabric tensor approach (Lee & Pietruszczak, 2008; Pietruszczak & Mroz, 2000) or the weakness plane approach (Jaeger, 1960).

3 CROSS-ANISOTROPIC CONSTITUTIVE MODEL

Reproducing the COx clay rock behaviour is envisaged by using a classical elasto-plastic constitutive law. A non-associated elasto-plastic Drucker-Prager yield criterion that allows for a parabolic strain hardening is used. Anisotropy is implemented initially for the elastic part (stiffness tensor adjusted to cross-anistropy) and eventually for the plastic part using the fabric tensor approach.

3.1 Drucker-Prager yield criterion

The yield surface definition is:

$$f\left(\sigma, \varepsilon_{eq}^{p}\right) = \sigma_{eq} + AI_1 - R\left(\varepsilon_{eq}^{p}\right) \tag{1}$$

$$A = \frac{2sin\varphi}{3 - sin\varphi} \tag{2}$$

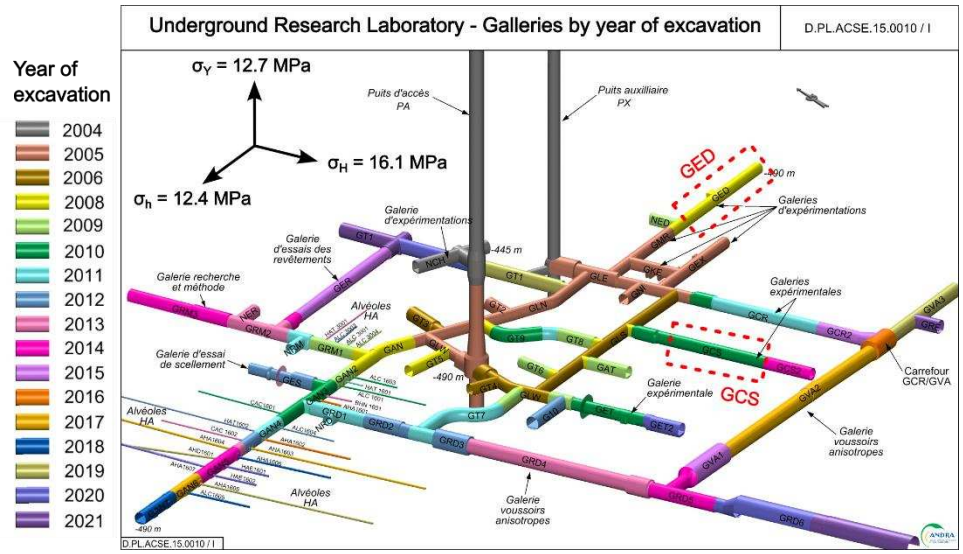

Figure 1. Meuse/Haute-Marne URL network (ANDRA 2019)

$$R\left(\varepsilon_{eq}^{p}\right) = \frac{6c\ cos\varphi}{3\ -\ sin\varphi} \quad (3)$$

where I_1 the first stress invariant, c is the material cohesion which is a function of the equivalent plastic strain and φ is the friction angle. The ε_{eq}^{p} is the equivalent plastic strain and the σ_{eq} the Von Mises equivalent stress which is defined as:

$$\sigma_{eq}\ =\ \sqrt{3J2}\ =\ \sqrt{\frac{3}{2}s_{ij}s_{ij}} \quad (4)$$

where s_{ij} are the components of the deviatoric part of the stress tensor and J_2 the second deviatoric stress invariant.

The parabolic hardening chosen on the cohesion introduces a dependence with ε_{eq}^{p} giving:

$$c\left(\varepsilon_{eq}^{p}\right) = c_0 + \frac{\left[\left(c_f - c_0\right)\varepsilon_{eq}^{p}\right]}{B_c\ +\ \varepsilon_{eq}^{p}} \quad (5)$$

where c_0 is the initial cohesion, c_f the final maximal cohesion after hardening and B_c is the equivalent plastic strain value for which half of the hardening of cohesion is attained.

A non-associated flow rule is generally required in the case of rocks, since the hypothesis of associativity over-estimates the material dilatancy. To better reproduce the COx clay rock behaviour, a non-associated flow rule is assumed:

$$g\left(\sigma, \varepsilon_{eq}^{p}\right) = \sigma_{eq} + \frac{2sin\psi}{3\ -\ sin\psi}I_1 - \frac{6c\ cos\psi}{3\ -\ sin\psi} \quad (6)$$

where ψ is the dilation angle.

3.2 Anisotropy of the shear strength

One of the most widely used methods for implementing material anisotropy, as proposed by Pietruszczak & Mroz (2000) and Pietruszczak et al. (2002), is the fabric tensor method. It consists of introducing a microstructure tensor A_{ij} able to describe the material fabric and thus to introduce orientation-dependent strength properties. In order to define the anisotropic parameters, the formulation is using a generalised unit loading vector which is defined as:

$$l_i = \frac{L_i}{\sqrt{L_k L_k}} \quad (7)$$

where L_i is the generalized loading vector:

$$L_i = \sqrt{\left(\tilde{\sigma}_{i1}^2 + \tilde{\sigma}_{i2}^2 + \tilde{\sigma}_{i3}^2\right)};\quad (i = 1,2,3) \quad (8)$$

where $\tilde{\sigma}_{ij}$ is the stress tensor expressed in the system of the bedding plane of angle θ as following:

$$\tilde{\sigma}_{ij} = R\sigma_{ij}R^T \quad (9)$$

where R is the matrix of rotation that depends on the angle θ and allows the change to the coordinate reference system linked to the bedding plane. Thus, the value of the angle θ has a significant effect on the results.

The projection of the microstructure tensor on the generalised unit loading vector l_i becomes:

$$\eta = \eta_0\left(1 + A_{ij}l_i l_j\right) \quad (10)$$

where η_o is a material parameter. The scalar variable η represents the anisotropic parameter and expresses the effect of load orientation relative to the material axes. The previous equation can be expressed considering higher order tensors, cross-anisotropic material structure and the use of cohesion as the anisotropic parameter as:

$$c_0 = \overline{c}\left(1 + A_{11}l_i l_j +\ b_1(A_{11}l_i l_j)^2 + b_2(A_{11}l_i l_j)^3\right) \quad (11)$$

where $\overline{c}$ is the cohesion under isotropic loading and A_{11}, b_1, b_2 are constant material parameters. Since c_0 is evolving relatively to the material fabric, it is more appropriate for the final cohesion c_f to evolve in the same manner as:

$$c_f\ =\ c_0\ \xi_c \quad (12)$$

where ξ_c is the ratio of the cohesion hardening.

For the parameters chosen, the evolution of the unconfined compressive strength (UCS) with bedding plane angle θ is presented in Figure 2.

Figure 2. UCS evolution with bedding plane angle

Since there are no experimental data available on the plastic behaviour of the COx claystone as a function of the bedding plane angle a calibration was realised based on similar rocks. The minimum value is reached between 40° and 50°, an observation consistent with other experimental observations for cross-anisotropic rocks (Haghighat & Pietruszczak, 2015; Niandou et al., 1997).

3.3 *Validation of the proposed cross-anisotropic constitutive law*

In order to verify the proposed cross-anisotropic constitutive law, a numerical modelling of a triaxial compression test is performed for different confining pressures (σ_3= 2 MPa, 5 MPa, 10 MPa, 20 MPa) and a bedding plane orientation of θ=90° (axial loading parallel to the bedding planes). A calibration of the parameters was realised with the goal of reproducing a plastic zone extent around the galleries that approximates the one observed in-situ. The calibrated parameters are $E_{//}$ = 5.5 GPa, $E_{\perp}$ = 4 GPa, $\nu_{//}$ = 0.25, $\nu_{\perp}$ = 0.3, $G_{//\perp}$ = 1.81 GPa, $\overline{c}$ = 1.4 MPa, ξ_c = 2.065, φ = 18°, ψ = 0°, A_{11} = 0.8, b_1 = 1.01, b_2 = 0.05. Results are presented in terms of deviatoric stress q vs axial strain ε_y (Figure 3).

Triaxial laboratory experiments were taken into account, however the values of the properties obtained from the calibration do not allow to reproduce the plastic zone extent observed around the galleries. Therefore, it is considered more appropriate to keep the values able to better characterize the large-scale response of the rock.

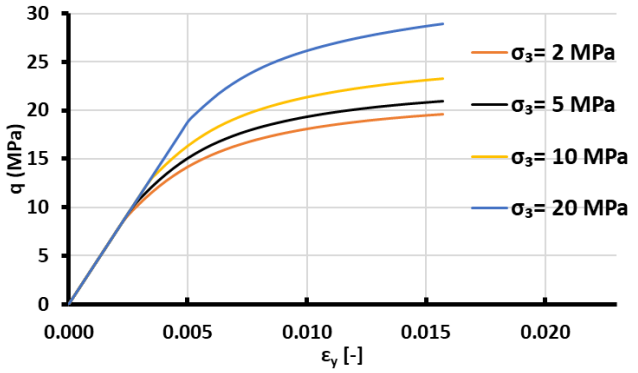

Figure 3. Triaxial compression numerical tests

4 NUMERICAL MODELLING OF GALLERY EXCAVATION

4.1 *Mesh, geometry, gallery orientation and stress state*

A large-scale three-dimensional numerical model of a single gallery excavation has been realised using the finite element solver Code Aster. The anisotropic constitutive law has been implemented using the code generator MFront (Helfer et al., 2015).

As illustrated in Figure 4(b), a circular gallery of 2.85 m radius is modelled and is located in the centre of a 114m x114m x 57m model. Half of the gallery has been modelled, assuming a symmetry with the vertical plane. The stratification of the rock is horizontal (dashed grey line) and the anisotropic in-situ stress state of the rock is considered. The initial stress state is consisting of three different values (Wileveau et al. 2007). In more detail, the vertical principal stress σ_v = 12.7 MPa, the minor horizontal principal stress σ_h = 12.4 MPa and the major horizontal principal stress σ_H = 16.1 MPa.

A purely mechanical analysis has been conducted without time effect. The mesh created in GMSH (Geuzaine & Remacle, 2009) is presented in Figure 4(a) and consists of approximately 250,000 hexahedron elements. Three different mesh zones of fineness were defined to improve the quality of the results in the vicinity of the gallery.

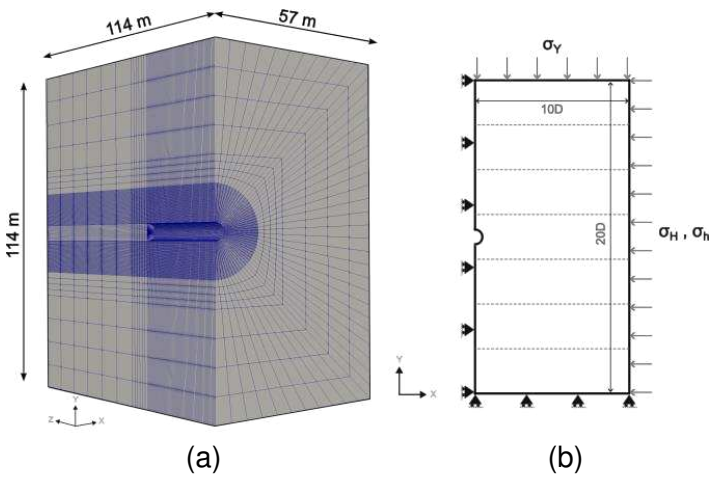

Figure 4. Proposed excavation model where (a) Mesh and (b) boundary conditions

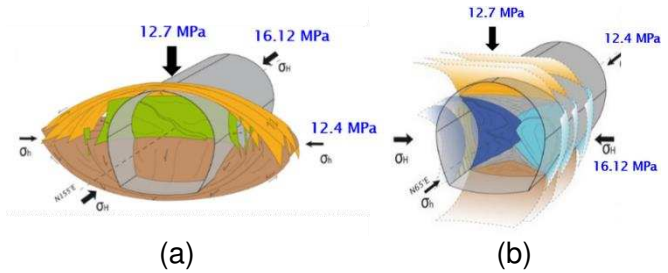

Figure 5. Conceptual model of excavation induced fractures for a) galleries //σ_H and b) galleries //σ_h (Armand et al., 2014)

An application to two of the Meuse/Haute Marne URL galleries has been performed, the GCS case (//σ_H) and the GED case (//σ_h). The location of the galleries is presented in Figure 1. A total of 40 m has been excavated using a stepwise removal of elements. Each element consists of a cylindrical volume of 1 m width. Concrete support has not been considered for this study. The

main difference concerning the two galleries lies mainly in their orientation regarding the major horizontal stress. This orientation in association with the COx rocks structural anisotropy can substantially affect the shape of the excavation induced fractures network around the gallery. Results presented in the next section will highlight the influence of the two counteracting phenomena in the generation of the plastic zone.

4.2 Results for the GCS gallery

The GCS gallery is parallel to the major principal stress (//σ_H) and is characterized by a quasi-isotropic stress state. For a standard isotropic constitutive law, an isotropic stress state would generally result into an isotropic circular extension of the plastic zone. Since the proposed model is considering the rock's anisotropy, a closer reproduction of what is observed in-situ is achieved in terms of the plastic extension. According to Armand et al. (2014), the extension of EDZ observed for a gallery parallel to the major stress is around 0.4D at the springline and about 0.15D at the crown and invert (Figure 5). In Figure 6(a) the plastic zone obtained numerically for the GCS gallery is presented. The extension after introducing anisotropy mainly develops horizontally reaching roughly 0.4D. Vertically the maximum value of extension is 0.1D. The EDZ extent observed in the URL is also presented in Figure 6 (dotted line) to allow for comparisons with the plastic zone calculated numerically.

Concerning convergences, as presented in Figure 7, for the GCS case a higher vertical convergence is obtained compared to the horizontal one. The in-situ data (Armand et al., 2013) prove the opposite. The difference between the horizontal and vertical convergence observed in-situ cannot be reproduced without the modelling of the fractures. This phenomenon will generate a substantially greater increase of the horizontal convergence for the GCS case.

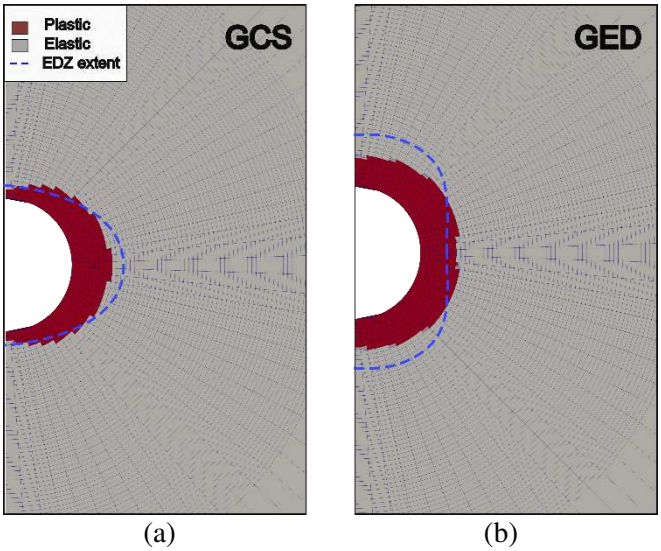

(a) (b)

Figure 6. Plastic indicator and in-situ measurements for (a) GCS and (b) GED galleries

4.3 Results for the GED gallery

For the GED gallery that is parallel to the minor horizontal stress (//σ_h), the anisotropic extent of the EDZ is observed in-situ to be less pronounced horizontally compared to the GCS gallery, since the initial stress state anisotropy is also affecting it. In this case, the stress state seems to be dictating the extension and reducing the horizontal preferential direction caused by the material anisotropy. The EDZ is reaching roughly 0.4D on the crown and invert and 0.2D on the springline.

Numerically, for the GED gallery as shown in Figure 6(b), an extension of 0.35D of the plastic zone is obtained around the gallery, leading to a slight under-estimation of the plastic zone extent on the crown and invert. Yet, the model is able to show how the two counteracting phenomena influence the plastic zone generated around the galleries.

In Figure 7, for the GED gallery the horizontal convergence is greater than the vertical one. Similar to the GCS gallery, this is not what is observed in-situ from Armand et al. (2013).

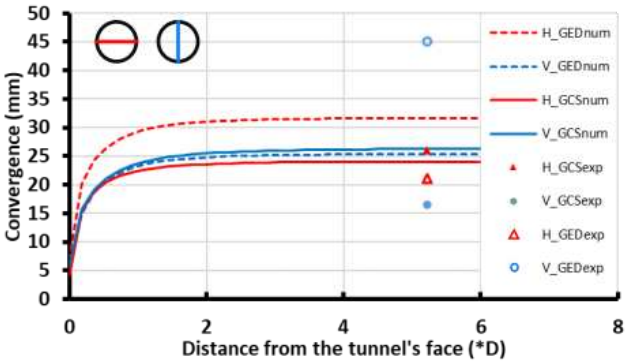

Figure 7. Numerical vertical and horizontal convergences for GCS and GED galleries

Numerical modelling of fractures and strain softening plasticity could potentially be considered for a better estimation of the convergences. Nevertheless, it could engender issues related to the numerical convergence, especially when combined with a complex geometry. Furthermore, an unsupported gallery case is modelled which consists of the worst possible scenario leading to a large extent of the EDZ. In the URL, most of the galleries are supported, convergences are reduced and the development of excavation-induced fractures is reduced.

5 CONCLUSIONS

This paper aims to propose an anisotropic constitutive elastoplastic law which is able to model the material anisotropy and to be applied to complicated three-dimensional geometries aiming at well characterizing the plastic zone around underground galleries after excavation. The model application on the COx claystone gives promising results compared to in-situ observations. This

confirms that the fabric tensor method can give accurate results.

The findings show the effect of structural anisotropy on the strength properties of the rock, mainly for the GCS gallery orientation for which a quasi-isotropic stress field pre-exists. For the GED gallery orientation, the plastic zone development and extent are due to the two counteracting effects (anisotropy and stress field).

Different future prospects such as enriching the model with more phenomena (including time-depending behaviour, damage framework, hydromechanical coupling etc.) are under investigation. The results obtained will contribute to underground engineering and safety.

6 ACKNOWLEDGEMENTS

The authors wish to gratefully thank ANDRA for funding this work through a doctoral contract.

7 REFERENCES

Abdi, H., Labrie, D., Nguyen, T. S., Barnichon, J. D., Su, G., Evgin, E., Simon, R., & Fall, M. 2015. Laboratory investigation on the mechanical behaviour of Tournemire argillite. *Canadian Geotechnical Journal*, **52(3)**, 268–282.

Abelev, A. V., & Lade, P. V. (2004). Characterization of Failure in Cross-Anisotropic Soils. *Journal of Engineering Mechanics*, **130(5)**, 599–606.

ANDRA 2019. *Synthesis of 20 years Research, Development and Demonstration in Andra's Underground Research Laboratory in Bure for Cigeo Project*. France Technical Document (p. 104).

Armand, G., Noiret, A., Zghondi, J., & Seyedi, D. M. 2013. Short- and long-term behaviors of drifts in the Callovo-Oxfordian claystone at the Meuse/Haute-Marne Underground Research Laboratory. *Journal of Rock Mechanics and Geotechnical Engineering*, **5(3)**, 221–230.

Armand, G., Leveau, F., Nussbaum, C., de La Vaissiere, R., Noiret, A., Jaeggi, D., Landrein, P., & Righini, C. 2014. Geometry and Properties of the Excavation-Induced Fractures at the Meuse/Haute-Marne URL Drifts. *Rock Mechanics and Rock Engineering*, **47(1)**, 21–41.

Code Aster 2017 EDF R&D, code général pour l'étude du comportement mécanique des structures diffusé sous licence GNU GPL

Delay, J., Vinsot, A., Krieguer, J.-M., Rebours, H., & Armand, G. 2007. Making of the underground scientific experimental programme at the Meuse/Haute-Marne underground research laboratory, North Eastern France. *Physics and Chemistry of the Earth*, Parts A/B/C, **32(1)**, 2–18.

Djouadi, I., Giot, R., Raude, S., Cuvilliez, S., Laigle, F., & Fernandes, R. 2020. Integration of Transverse Isotropy in the Instantaneous Behaviour of Geomaterials with Application to Numerical Modelling of Underground Structures. *Geotechnical and Geological Engineering*, **38(5)**, 4917–4938.

Geuzaine, C., & Remacle, J.-F. 2009. Gmsh: A 3-D finite element mesh generator with built-in pre- and post-processing facilities. *International Journal for Numerical Methods in Engineering*, **79(11)**, 1309–1331.

Haghighat, E., & Pietruszczak, S. 2015. On the mechanical and hydraulic response of sedimentary rocks in the presence of discontinuities. *Geomechanics for Energy and the Environment*, **4**, 61–72.

Helfer, T., Michel, B., Proix, J.-M., Salvo, M., Sercombe, J., & Casella, M. 2015. Introducing the open-source mfront code generator: Application to mechanical behaviours and material knowledge management within the PLEIADES fuel element modelling platform. *Computers & Mathematics with Applications*, **70(5)**, 994–1023.

Jaeger, J. C. 1960. Shear failure of anisotropic rocks. *Geological Magazine*, **97(1)**, 65–72.

Lade, P. V. 2007. Modeling failure in cross-anisotropic frictional materials. *International Journal of Solids and Structures*, **44(16)**, 5146–5162.

Lee, Y.-K., & Pietruszczak, S. 2008. Application of critical plane approach to the prediction of strength anisotropy in transversely isotropic rock masses. *International Journal of Rock Mechanics and Mining Sciences*, **45(4)**, 513–523.

Nasseri, M. H. B., Rao, K. S., & Ramamurthy, T. 2003. Anisotropic strength and deformational behavior of Himalayan schists. *International Journal of Rock Mechanics and Mining Sciences*, **40(1)**, 3–23.

Nguyen, T. S., & Le, A. D. 2015. Development of a constitutive model for a bedded argillaceous rock from triaxial and true triaxial tests. *Canadian Geotechnical Journal*, **52(8)**, 1072–1086.

Niandou, H., Shao, J. F., Henry, J. P., & Fourmaintraux, D. 1997. Laboratory investigation of the mechanical behaviour of Tournemire shale. *International Journal of Rock Mechanics and Mining Sciences*, **34(1)**, 3–16.

Pardoen, B., Seyedi, D. M., & Collin, F. 2015. Shear banding modelling in cross-anisotropic rocks. *International Journal of Solids and Structures*, **72**, 63–87.

Parisio, F., Samat, S., & Laloui, L. 2015. Constitutive analysis of shale: A coupled damage plasticity approach. *International Journal of Solids and Structures*, 75–76, 88–98.

Pietruszczak, S., & Mroz, Z. 2000. Formulation of anisotropic failure criteria incorporating a microstructure tensor. *Computers and Geotechnics*, **26(2)**, 105–112.

Pietruszczak, S., Lydzba, D., & Shao, J. F. 2002. Modelling of inherent anisotropy in sedimentary rocks. *International Journal of Solids and Structures*, **39(3)**, 637–648.

Souley, M., Vu, M.-N., & Armand, G. 2022. 3D Modelling of Excavation-Induced Anisotropic Responses of Deep Drifts at the Meuse/Haute-Marne URL. *Rock Mechanics and Rock Engineering*, **55(7)**, 4183–4207.

Tsang, C.-F., Bernier, F., & Davies, C. 2005. Geohydromechanical processes in the Excavation Damaged Zone in crystalline rock, rock salt, and indurated and plastic clays-In the context of radioactive waste disposal. *International Journal of Rock Mechanics and Mining Sciences*, **42(1)**, 109–125.

Wileveau, Y., Cornet, F.H., Desroches, J., & Blumling, P. 2007. Complete in situ stress determination in an argillite sedimentary formation. *Physics and Chemistry of The Earth*, **32**, 866-878.

Zhang, C.-L., Armand, G., Conil, N., & Laurich, B. 2019. Investigation on anisotropy of mechanical properties of Callovo-Oxfordian claystone. *Engineering Geology*, **251**, 128–145.